



ELSEVIER

15 January 1997

OPTICS
COMMUNICATIONS

Optics Communications 134 (1997) 281–288

Full length article

Tolerant design of a planar-optical clock distribution system

Barbara Lunitz, Jürgen Jahns

FernUniversität Hagen, Lehrgebiet Optische Nachrichtentechnik, Feithstr. 140, D-58084 Hagen, Germany

Received 26 April 1996; accepted 2 August 1996

Abstract

This paper describes a tolerant design for a planar optical clock distribution system. It uses a correction optics that consists of a sequence of lenses at regular distances similar to a lens waveguide. The correction optics greatly reduces detrimental effects due to the influence of substrate tolerances, variations of the wavelength and the temperature on the light propagation. Ray-tracing simulations are used to analyze the performance of the corrected system. Practical considerations for the design of the overall system are presented.

Keywords: Optical clock distribution; Planar optics; Optical design; Microoptics

1. Introduction

For long and medium distances, optical communications has become dominant over conventional electric communications. However, for short distances, as they occur for example within a computer, optical interconnections have not yet been able to replace metallic wires. One of the main reasons for this are difficulties with the packaging of the optics. On the other hand, with increasing the scale and speed in VLSI circuits chips, conventional electrical interconnects become problematic [1]. The problems of electronic communications are limitations of the temporal bandwidth due to capacitances, crosstalk due to inductivities as well as physical effects like electromigration due to the scaling-dependent increase of the current density. These effects are particularly troublesome for intra- and inter-chip clock distribu-

tion where high speed and relatively long distances are required.

The use of optical interconnections allows one to solve these problems and to achieve a higher data rate, interconnection density [2], immunity against electromagnetic interference, and lower energy requirements [3]. On the other hand, electrical interconnects have the advantage of a well known and cheap technology whereas conventional opto-mechanic packaging is expensive and not adequate for VLSI electronics. In order to remove the shortcomings of optics, it is therefore necessary to use micro-optic fabrication and packaging techniques. Planar optics [4] was suggested as a means to integrate free-space optical systems using standard lithographic fabrication.

This article deals with planar optical clock distribution. In particular, we consider clock distribution

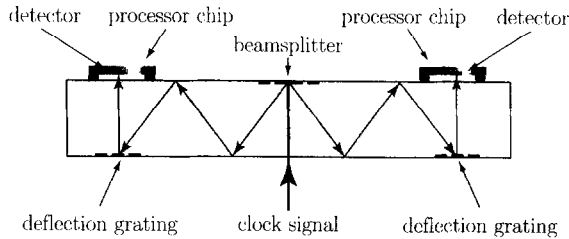


Fig. 1. Principle of the clock distribution system with two processor chips using an H-tree configuration.

to the chips of a multiprocessor system. The clock signal is used to synchronize the communication of and the communication between the processors. The clock frequency might, for example, be on the order of 1 GHz. The distances for the clock signal depend on the size and spacing of the chips. For a wafer scale system, the distances might be on the order of 100 mm. The principle of a planar optical clock distribution system was suggested and demonstrated in Ref. [5]. A modulated laser beam enters a substrate and is split up by using a cascade of 1×2 beamsplitters. These are implemented as binary phase gratings with a sufficiently small period to suppress all but the two first orders. Following a zig-zag path through the substrate, the light beam passes a system of beamsplitter and beam deflection gratings (Fig. 1) arranged as an H-tree. The deflection gratings have the same period as the beam splitters and are used to make the light beam hit the beamsplitter gratings normally. After a cascade of N 1×2 -beamsplitters the input beam is split up into 2^N output beams.

At the output positions, detectors convert the optical signals into electrical clock signals. Ideally, the light beams are supposed to be in register with the detector positions resulting in the same light intensity at the various detectors therefore yielding proper timing. However, several effects influence the path of the light beam traveling inside the substrate and can cause a lateral and/or angular offset of the beam. Such an offset will generally result in a drop of the detected light intensity. This effectively results in a skew of the detected electrical signal and hence in a nonuniformity of the clock signals at the various output positions. In the worst case, the offset may be so large that the light beam does not hit the detector area at all. It is obvious that the effects of an offset

will become more severe as one goes to large substrates as it might be of interest for chip-to-chip interconnects in optical multichip modules [6] or for board-to-board interconnects [7].

The various sources for error are (a) a tolerance of the substrate thickness h , (b) a wedge between the substrate surfaces represented by an angle α , (c) a tolerance of the wavelength λ of the light beam, and (d) a tolerance of the ambient temperature T . An analysis of the influence of these tolerances on the stability of the light propagation has been given in Ref. [8] and also recently by Yeh and Kostuk [9].

In this article, we are going to present a solution to the problem that is based on a tolerant optical design of the clock distribution system. The virtue of a tolerant design is the fact that one can accept large tolerances of the substrate parameters and the operating parameters wavelength and temperature. The larger the variations, the lower the cost for the system and the better the performance.

This article is organized as follows: the principle of a tolerant design is presented in Section 2. An analysis of the effect of the aforementioned tolerances (a)–(d) is given in Section 3. The performance of the tolerant clock distribution system is analyzed by ray tracing simulations (Section 4). The results

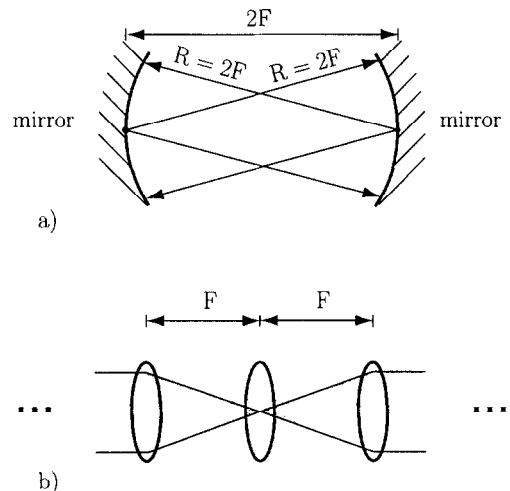


Fig. 2. (a) Confocal resonator with convex mirrors. (b) Unfolded arrangement of lenses. It might be interesting to note that an infinite sequence of such lenses can be considered as a "lens waveguide" [11,12].

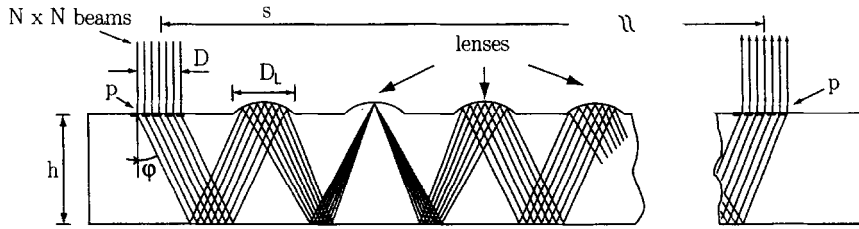


Fig. 3. Optical substrate with correction optics. The lenses are separated by one focal length. (h - substrate thickness, p - grating period, φ - propagation angle, d - beam width, D_L - lens diameter, s - lateral beam position).

are used to compare the corrected tolerant with the uncorrected system. A few practical issues of the implementation will be discussed in Section 5. In Section 6 three different lens designs are compared for the suitability in planar optics.

2. Tolerant clock distribution system

In order to build a tolerant optical system that warrants stable light propagation we use an analogy with a laser resonator. In the simplest case of a laser resonator with two plane mirrors even a small longitudinal or angular offset between the mirrors can result in a walkoff of the partial beams and hence prevent the resonator from lasing. In order to improve the stability of a laser, other mirror configurations are used [10]. The most stable laser configuration is the confocal laser resonator where two convex mirrors are placed two focal lengths apart (Fig. 2a). The lens action of the mirrors tends to "pull back" the light beam whenever it walks off its ideal path because of a possible misalignment.

We adapt this concept to our clock distribution system by placing a series of lenses in the path of the light beam. The lenses all have the same focal length F and are separated along the direction of light propagation by a distance F (Fig. 2b). In a planar optical configuration, the separation of the lenses is related to the substrate thickness h and the propagation angle φ by $F = 2h/\cos\varphi$ (Fig. 3). The lenses can be implemented either as diffractive-reflective or purely reflective micro-optic elements. In the following, we will refer to the lens diameter as D_L . s denotes the lateral position of the light beam. It is assumed that the light beam is coupled into and out

of substrate using a grating of period p . The width of the input beam is D .

3. Effects of tolerances

In this section, we present an analytical treatment of the tolerances that occur in an uncorrected clock distribution system. As we mentioned earlier instability of the light propagation is a result of tolerances or variations of the following four parameters:

- $h \pm \Delta h$ substrate thickness
- $\Delta\alpha$ wedge between the substrate surfaces
- $T \pm \Delta T$ temperature
- $\lambda \pm \Delta\lambda$ vacuum wavelength

In the ideal case, Δh , $\Delta\alpha$, ΔT , and $\Delta\lambda$ are all zero. In the nonideal case, a lateral and angular offset will result as indicated by Fig. 4. The lateral path of the light beam is denoted by s . In the following, we present without derivation simple equations for the lateral offset Δs of the light beam for each of the four cases where we assume just one tolerance to be nonzero.

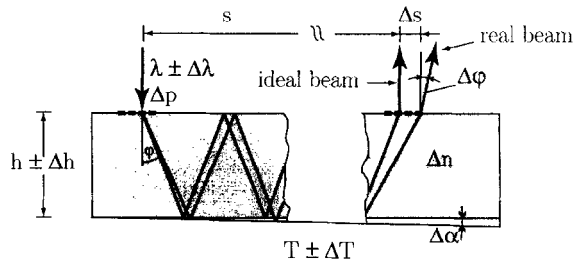


Fig. 4. Effect of tolerances on the optical beam.

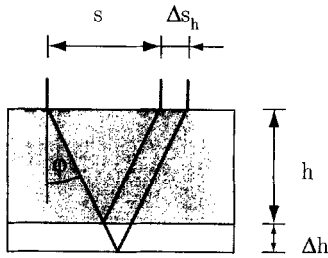


Fig. 5. Effect of substrate thickness variation Δh after one reflection.

(a) $\Delta h \neq 0$: As shown in Fig. 5, a thickness tolerance Δh causes a lateral offset Δs_h after one double pass of the light through the substrate:

$$\Delta s_h = 2 \Delta h \tan \varphi. \tag{1}$$

Here φ is the angle under which the light travels inside the substrate. φ is determined according to the equation:

$$\sin \varphi = \frac{\lambda}{(np)}, \tag{2}$$

where n is the refractive index of the substrate and p is the period of the beam splitter gratings.

Obviously, for this case, no change of the beam's angular direction occurs:

$$\Delta \varphi_h = 0. \tag{3}$$

(b) $\Delta \alpha \neq 0$: A wedge $\Delta \alpha$ causes a change of the angle under which the light propagates:

$$\Delta \varphi_\alpha = 2 \Delta \alpha. \tag{4}$$

This effect results in an exponential growth of the lateral offset for multiple bounces since the angular offset doubles after every reflection.

(c) $\Delta T \neq 0$: A temperature change will cause various effects. In addition to a variation of the dimensions of the substrate expressed by

$$\frac{\Delta h}{h} = k_1 \Delta T, \tag{5}$$

there will be a change of the refractive index n according to

$$\frac{\Delta n}{n} = k_2 \Delta T. \tag{6}$$

k_1 and k_2 are the linear thermal expansion coefficient and the thermal coefficient of the refractive index, respectively. Both effects cause a variation of the angle under which the light beam propagates since $\sin \varphi = \lambda / [(n \pm \Delta n)(p \pm \Delta p)]$. For the tolerance in φ we can write $\Delta \varphi / \Delta T = -(k_1 + k_2) \tan \varphi$. The lateral offset due to the temperature change is

$$\Delta s_T = 2 h \tan \varphi \left(k_1 \Delta T - \frac{k_1 \Delta T + k_2}{\cos^2 \varphi} \right), \tag{7}$$

$$\Delta \varphi_T = -(k_1 + k_2) \tan \varphi \Delta T. \tag{8}$$

(d) $\Delta \lambda \neq 0$: A wavelength tolerance that may be caused by either fabrication tolerances of the laser diode or by a temperature drift influences the angle under which the light is coupled into the substrate according to Eq. (2). For our analysis we assume monochromatic light of wavelength λ . The lateral displacement of the beam for $\Delta \lambda \neq 0$ is

$$\Delta s_\lambda = 2 h \frac{\tan \varphi \Delta \lambda}{\cos^2 \varphi \lambda}. \tag{9}$$

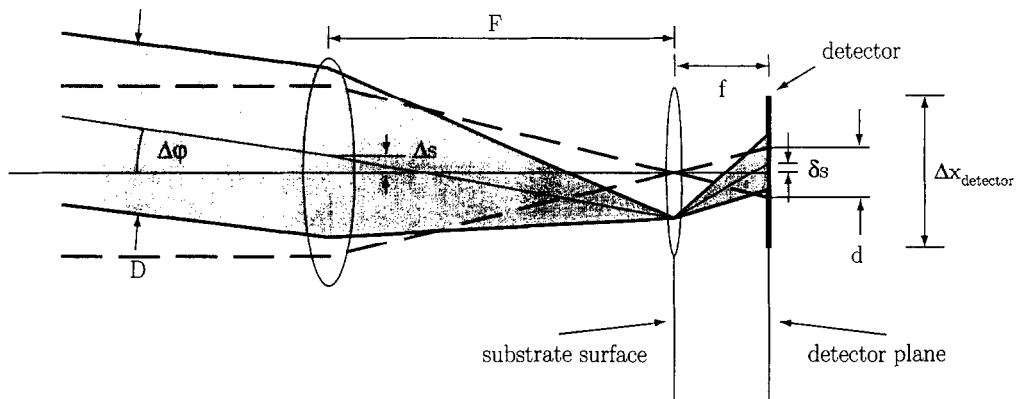


Fig. 6. Effects of the lateral and angular offset on the beam. The ideal case (no offset) is represented by the dashed line.

The angular offset is

$$\Delta\varphi_\lambda = \frac{\Delta\lambda}{\lambda} \tan\alpha. \tag{10}$$

It is important to consider how such a lateral and angular offset affects the detected light signal. For this end we consider in more detail the optics near the detector. We assume that the correction system is designed in such a way that the last lens in the sequence focuses the light beam onto the detector (Fig. 6). The function of the second lens in Fig. 6 will be discussed in detail in Section 5. A lateral and angular offset of the light beam results in a loss of detected optical power. The lateral offset leads to power loss in the case of:

$$D/2 + \Delta s > D_L/2, \tag{11}$$

with D diameter of the beam and D_L diameter of the lens.

A beam displacement in the detector plane caused by the angular offset is given by $\Delta s_{\text{angular}} = F \tan \Delta\varphi$. For this offset power loss occurs if

$$\Delta s_{\text{angular}} > \Delta x_{\text{detector}}/2, \tag{12}$$

respectively. Using a detector with a large area increases the misalignment tolerances, but on the other hand the detector size is limited by its capacitance which determines the bandwidth of the receiver. For high speed applications like the clock distribution system the detector area has to be small. Keeping the detector size at a minimum is also required by the economics of integration.

4. Simulation

4.1. Model

The physical system that we analyze is shown in Fig. 3. It consists of two gratings for coupling the light beam into and out of the substrate and a series of lenses for correcting the light propagation. The analysis was performed using a ray tracing simulation. The optical input to the system is represented by a 2-D array of $N \times N$ parallel input beams impinging onto the substrate at normal incidence. In our case, $N = 9$. The lateral pitch in the input array is $125 \mu\text{m}$ resulting in an overall width d of the

illuminating beam of $1 \text{ mm} \times 1 \text{ mm}$. The lenses have a focal length $F = 2h/\cos\varphi$ and are assumed to have circular shapes with a diameter of D_L . Several lens designs were tested as discussed in Section 6. For the simulations shown is this section lenses with elliptical phase profiles were assumed (see Eq. (19), Section 6) which yield better results than other designs [13,14].

Every ray is traced through the system and its output position s_{ij} is determined. The lateral center position of the beam is then calculated according to

$$s = \frac{1}{N^2} \sum_{ij} s_{ij}, \tag{13}$$

with $i, j = 1, \dots, N$.

The lateral offset from the ideal position is then given as

$$\Delta s = s - s_{\text{ideal}}. \tag{14}$$

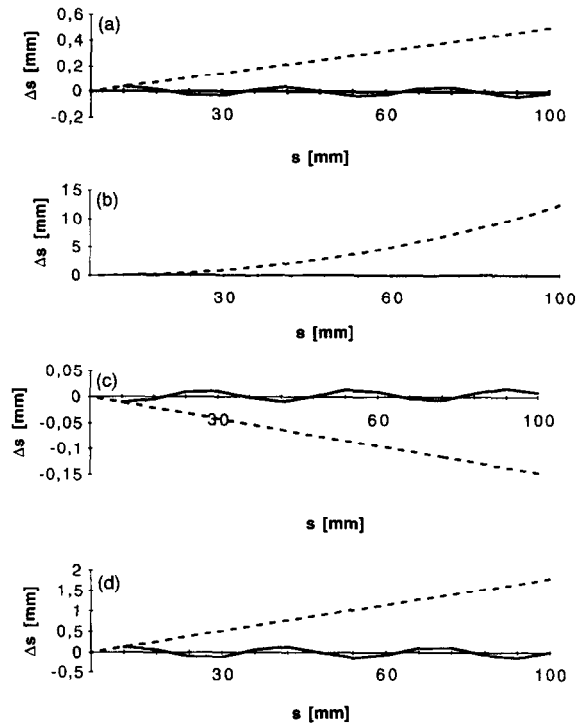


Fig. 7. Simulation results: Lateral offset Δs as a function of the lateral position s for (a) deviation of thickness $\Delta h: 25 \mu\text{m}$; (b) wedge between the surfaces $\Delta\alpha: 1'$; (c) deviation of temperature $\Delta T: 100 \text{ K}$; (d) wavelength shift $\Delta\lambda: 10 \text{ nm}$.

For the simulation the following parameters were chosen: $h = 5000 \mu\text{m}$, $\Delta h = 25 \mu\text{m}$, $\Delta\alpha = 1'$, $\Delta T = 100^\circ\text{C}$, $\lambda = 0.85 \mu\text{m}$, $\Delta\lambda = 0.01 \mu\text{m}$.

Furthermore we choose: $D = 1 \text{ mm}$, $D_L = 2 \text{ mm}$, $p = 1 \mu\text{m}$, $n = 1.46$.

From this follows that in the ideal case the coupling angle is $\varphi = 35.6^\circ$.

4.2. Simulation results

The following curves (Figs. 7a–d) show the results of the simulations for each of the four cases discussed above. On the abscissa the lateral position of the beam is shown up to a distance of 10 cm. This value corresponds to a reasonable wafer size as it might be of interest for an optical multiprocessor system. On the ordinate the lateral offset Δs is given. In all four cases, the lateral offset is shown for the uncorrected and the corrected system.

As it can be seen, the strongest influence in the uncorrected system is the wedge error since it grows exponentially (Fig. 7b). In this case, the lateral offset becomes so large that it would not be practical to use substrate mode interconnects unless one controls the substrate parameters very carefully. Although the other tolerances have a much less drastic effect they, too, can severely reduce the amount of light at the detector.

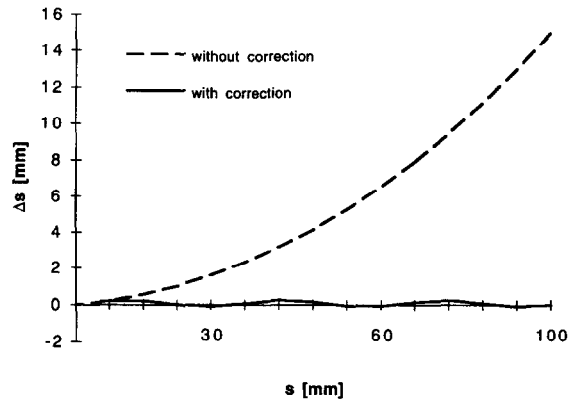


Fig. 8. Lateral offset Δs with all tolerances present. The same values as in Fig. 7 were used.

For the corrected system, the error in the lateral position is significantly reduced to a practical level of a few hundred micrometers. Even in the case of all tolerances combined (Fig. 8) we can see that the offset stays within a window of $\pm 175 \mu\text{m}$.

Besides the lateral offset of the beam there also occurs an angular offset. Fig. 9 shows the angular offset for the the uncorrected and the corrected system, for values $\Delta\alpha = 2'$, $\Delta\alpha = 1'$, and $\Delta\alpha = 0.5'$ (solid line, dashed line, and fine dashed line) of the wedge between the substrate surfaces. The angle $\Delta\varphi$ in the uncorrected system increases linearly as ex-

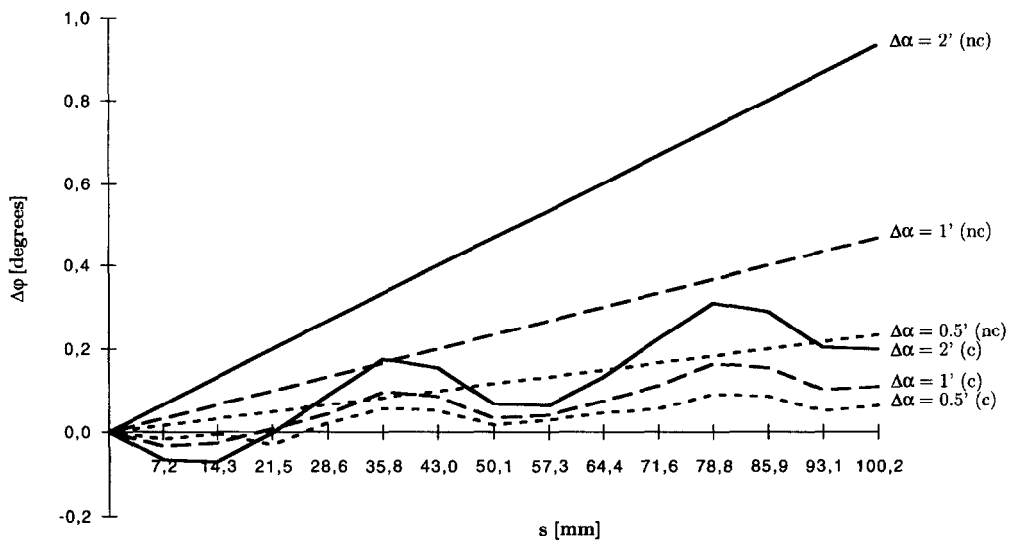


Fig. 9. Angular offset $\Delta\varphi$ as a function of different values of $\Delta\alpha$. c – with correction optics; nc – without correction optics.

pected in Eq. (4). For the corrected system we observe a reduction. It is interesting to note the oscillation of the actual position around the ideal position due to the action of the correcting system (see next section). The curves for the other three cases (Δh , $\Delta \lambda$, ΔT) are not shown here but they look similar to the results of Fig. 9.

The curves shown in Figs. 7a–d allow one to determine tolerance ranges for the four quantities that we have considered. For example, if we request to keep the lateral offset Δs smaller than $100 \mu\text{m}$ the tolerances and variations have to be kept within the following limits:

$$\begin{aligned} \Delta h < 38 \mu\text{m}, \quad \Delta \alpha < 0.17^\circ, \\ \Delta T < 1000 \text{K}, \quad \Delta \lambda < 5 \text{nm}. \end{aligned}$$

We would like to note, that we have neglected any widening of the beam due to diffraction. As long as the width of the beam is large enough, diffraction effects are small [5]. This is the case in our simulation where the width of the beam is 1mm and the wavelength is $\lambda/n \approx 0.58 \mu\text{m}$.

5. Practical considerations

Although the correction optics greatly improves the performance of the clock distribution system, we have to consider if it is sufficient for our purposes. For example, for high speed applications, it is necessary to use photodetectors with a small photosensitive area with a diameter $\Delta x_{\text{detector}} \leq 100 \mu\text{m}$. The detectors are located at well-defined positions. Therefore, the lateral offset of the output beams and their diameters are sufficiently small. Our clock distribution system uses dimensions that justify a description based on geometrical optics. Due to the effect of the sequence of lenses, a light beam that is collimated in one plane will be focused after two double passes through the substrate (Fig. 3). In a plane, where the beam is collimated, it has a diameter D , a lateral offset Δs , and an angular offset $\Delta \varphi$ (Fig. 6). From our simulation results we see that in the worst case $\Delta s \approx \pm 170 \mu\text{m}$ and $\Delta \varphi \approx 0.8^\circ$. We mentioned before, that the beam diameter is quite large, typically $D \approx 1000 \mu\text{m}$. Since D is much larger than $\Delta x_{\text{detector}}$, we cannot place the photodetector in a plane where the beam is collimated,

because most of the light energy would be wasted. In the next plane, where the beam is focused, its diameter will be $[2(\lambda/n)F]/D \approx 14 \mu\text{m}$ using the values of Section 4. Its lateral offset is $F \tan \Delta \varphi \approx 172 \mu\text{m}$ for the maximum value of $\Delta \varphi$. Although the spot size would be small enough, the lateral offset would be too large.

To reduce the beam size and offset in the detector plane, we use a field lens of focal length f in the plane where the beam is focused (Fig. 6). It is assumed that the field lens is positioned on the surface of the glass substrate a distance f away from the photodiode. f is assumed to be much smaller than F , a typical value would be $f = 500 \mu\text{m}$. In the plane of the photodetector, the beam will now be offset by

$$\begin{aligned} \delta s = F \tan \Delta \varphi \left(1 - \frac{1}{\cos \Delta \varphi} \right) + f \tan \Delta \varphi \\ + \left[\left(1 - \frac{1}{\cos \Delta \varphi} \right)^2 - \frac{f}{F} \cos \Delta \varphi \right] \Delta s. \end{aligned} \quad (15)$$

Δs and $\Delta \varphi$ alternate between two extreme values, however with a phase difference. Therefore, the worst case for both does not occur for the same value of s . Using the value $\Delta s = 167 \mu\text{m}$ and the corresponding angular offset $\Delta \varphi = 0.33^\circ$ we obtain $\delta s \approx 4 \mu\text{m}$.

The diameter of the beam in the detector plane is given as

$$d = fD/F. \quad (16)$$

With the values given above $d \approx 40 \mu\text{m}$. The diameter of the detector $\Delta x_{\text{detector}}$ has to be large enough so that $\Delta x_{\text{detector}} \geq \delta s + d$. In our particular example, $\Delta x_{\text{detector}} \geq 44 \mu\text{m}$.

6. Lens design considerations

The lenses used in the correction system can be designed in different ways. For our system we tried three designs: circular (c), elliptical symmetric (s), and elliptical asymmetric (a) lenses. The phase profiles of these lenses are described by the following equations:

$$\phi_c(x, y) = - \left(\frac{2\pi n}{\lambda} \right) \left(\sqrt{x^2 + y^2 + F^2} - F \right), \quad (17)$$

$$\phi_a(x, y) = -\left(\frac{2\pi n}{\lambda}\right) \times \left(\sqrt{(x + F \sin \alpha)^2 + y^2 + (F \cos \alpha)^2} - F + x \sin \alpha\right), \quad (18)$$

$$\phi_s(x, y) = -\left(\frac{\pi n}{\lambda}\right) \left(\sqrt{x^2 + y^2 + 2xF \sin \alpha + F^2} + \sqrt{x^2 + y^2 - 2xF \sin \alpha + F^2} - 2F\right). \quad (19)$$

Eq. (17) represents a lens with circular symmetry. Eq. (18) describes an asymmetric lens that collimates a tilted plane wave [15]. For this case the direction of incidence is important, so that the correction system consists of an alternating sequence of asymmetric lenses. Finally, Eq. (19) describes a symmetric lens which is obtained as the superposition of two asymmetric lenses [15].

We used all three design types for the ray tracing simulations and the results were compared. With ray tracing simulations we observed that the lenses with the circular phase profile produce worse results than the other two designs. The design with the symmetric lenses yielded slightly better results than the asymmetric lenses.

7. Conclusion

A tolerant design for a planar optical clock distribution system was proposed and analyzed. It uses a sequence of reflective lenses positioned at regular positions on the surface of the substrate. Using ray tracing simulations, we compared the performance of the corrected system with the uncorrected clock distribution system. Significant improvement in the position of the beam can be achieved even for relatively large variations of the substrate thickness,

non-parallelism of the substrate surfaces, wavelength and temperature. A directional offset of the output beam can be further minimized by a field lens at the end of the optical system.

The results presented here are based on geometric optics considerations. Another extension of our model that is of interest is the analogue of the "lens waveguide" [11] that is based on the wave propagation of Gaussian beams. Further questions are also of interest. For example, we plan to consider issues like the influence of different spacings of the lenses and different implementations of the lenslets (diffractive-reflective or purely reflective), the receiver design, etc. These issues are relevant when it comes to a practical implementation of the system.

References

- [1] J.W. Goodman, F.I. Leonberger, S. Kung and R.A. Athale, *Proc. IEEE* 72 (1984) 850.
- [2] J.E. Midwinter, *Photonics in Switching*, Vol. I (Academic Press, New York, 1993).
- [3] M.R. Feldman, S.C. Esener, C.C. Guest and S.H. Lee, *Appl. Optics* 27 (1988) 1742.
- [4] J. Jahns and A. Huang, *Appl. Optics* 28 (1989) 1602.
- [5] S.J. Walker and J. Jahns, *Optics Comm.* 90 (1992) 359.
- [6] B. Acklin and J. Jahns, *Appl. Optics* 33 (1994) 1391.
- [7] H.J. Haumann, H. Kobolla, F. Sauer, J. Schmidt, J. Schwider, W. Stork, N. Streibl and R. Völkel, *Opt. Eng.* 30 (1991) 1620.
- [8] J. Jahns, *Tolerant design of planar optical interconnections*, *OSA Proc. Intern. Optical Design Conference*, Vol. 22 (1994).
- [9] J.-H. Yeh and R.K. Kostuk, *J. Lightwave Techn.* 13 (1995) 1566.
- [10] A.E. Siegman, *Lasers* (University Science Books, Mill Valley, CA, 1986).
- [11] J. Hirano and Y. Fukatsu, *Proc. IEEE* 52 (1964) 1284.
- [12] H.D. Wu and F.S. Barnes, *Microlenses, Coupling Light to Optical Fibers* (IEEE Press, 1990).
- [13] J. Jahns and S.J. Walker, *Appl. Optics* 7 (1990) 931.
- [14] S.J. Walker and J. Jahns, *J. Opt. Soc. Am.* 7 (1990) 1509.
- [15] J. Jahns and B. Acklin, *Optics Lett.* 18 (1993) 1594.